PCCP

Accepted Manuscript

ROYAL SOCIETY OF CHEMISTRY

www.rsc.org/pccp

Explicit calculation of the excited electronic states of the photosystem II reaction centre

Terry J. Frankcombe*

Research School of Chemistry, Australian National University, ACT 0200 Australia

Abstract

The excited states of sets of the cofactors found in the photosystem II reaction centre have been calculated directly as a multi-monomer supermolecule for the first time. Time-dependent density functional theory was used with the CAM-B3LYP functional. Multiple excited states for each cofactor were found at lower energies than the lowest energy state corresponding to charge transfer states (in which an electron is shifted from one cofactor to another). The electrostatic environment was found to have a dramatic impact on the excited state energies, with the effect of a surrounding dielectric medium being less significant.

*E-mail: tjf@rsc.anu.edu.au

1 Introduction

Photosynthesis is vital to life on Earth, directly converting solar energy into chemical energy. In green plants photosynthesis begins in photosystem II (PS II), in which energy from adsorbed photons creates electron-hole pairs in the PS II reaction centre. This primary charge separation provides the potential to oxidise water to O_2 and feeds electrons to subsequent photosynthetic reactions.[1,2] Correspondingly, PS II has been the subject of a large body of international research. While its importance inspires fundamental interest, many have sought to understand the operation of PS II in order to design biomimetic solar energy devices.[3]

Of particular interest is the mechanism of primary charge separation in the PS II reaction centre.[4] In recent years efforts have been made to model the kinetics of charge separation within the PS II reaction centre.[5–11] While a range of approaches have been applied to formulate charge transfer models, the parameters for the modelling generally come either from empirical fitting to experimental data or from calculations of excited state coupling parameters based on chlorophyll monomer data. While couplings based on older dipole representations[12] have been used in some modelling,[6] distributed partial charges designed to accurately reproduce the electrostatic fields around excited monomers have recently become available[13,14] and have been used in more recent modelling.

Continuous improvements in algorithms and increases in the computing power regularly available mean that treating aggregates of photosynthetic cofactors directly in a single electronic structure theory calculation is now achievable. Steps have been made towards explicit calculations of bacteriochlorophylls clustered with carotenoids[15] and "divide and conquer" approaches have been used.[16] Bac-

terial and light harvesting complexes have been studied in some detail (see Ref. 17 for a recent review) and comprehensive and accurate effective Hamiltonian models have been built for photosystem I.[18] However, there has been a dearth of calculations that treat multiple PS II cofactors as a fully coupled aggregation with an unbiased treatment of their electronic structure. Steps in this direction are made in the current study, with explicit calculation of the excited electronic states of the combined cluster of the PS II reaction centre cofactors that are thought to be involved in charge separation within density functional theory with long-range correction.

2 Methods

All calculations were performed with Gaussian 09.[19] Time-dependent DFT calculations (TDDFT) were performed using the CAM-B3LYP functional[20,21] using a number of basis sets ranging from 6-31G to 6-31+G(d,p). The CAM-B3LYP functional was selected as it has been reported to give a good description of excited states for chlorophyll-like systems and for charge transfer states in general.[18,20–23]

The effect of a polarisable medium was investigated using the PCM model[24] for non-equilibrium excitation. A water-like van der Waals radius cavity was used for all considered relative permeabilities (dielectric constant).

Atomic coordinates of the PS II reaction centre were taken from the 1.9 Å resolution crystal structure of Umena *et al.*[25], with hydrogen atoms added to saturate the structures. In benchmarking calculations the chlorophyll structures, including side chains, were used, usually with the long chlorophyll hydrocarbon tail truncated at the contained ester to yield a tail terminated with carboxylic acid. Other

calculations used structures built from idealised cofactors, combined into a "supermolecule". For the latter the centres of the rings of the cofactors were identified from the crystal structure data, along with the locations of two other landmark features in each cofactor. Idealised cofactor structures (at their optimised geometries) were then aligned with these landmark points to create the idealised structure. For chlorophyll and pheophytin the idealised cofactor structure was a chlorin ring with an additional five membered ring and ketone at the C13-C15 position, as found in chlorophyll. The ketone was used as the second landmark for orienting the rings, with the adjacent aliphatic carbon atom being the third landmark. The central Mg atom was included at the centre of the chlorin ring for the chlorophyll idealisation. For plastoquinone the idealised structure was benzene substituted with three methyl and two ketone groups, with the inter-ketone axis and benzene plane used for orientation.

The character of each excited state was identified by examining the orbitals describing the transition from the ground state.

It is useful to be precise about the terminology being used in this paper. Two distinctly different types of excited states are considered here. These are illustrated in Figure 1, which shows an orbital occupation diagram for two hypothetical cofactor monomers, A and B. Four orbitals are shown for each monomer, being the highest two occupied and lowest two unoccupied orbitals of the ground state of the isolated monomer. The upper panel shows the ground state, which in this case is the same configuration whether the monomers are treated independently or as an AB supermolecule. The first type of excitation being discussed is shown in the middle panel, in which an electron gets excited from the HOMO of a monomer to the LUMO of the same monomer. This is termed a local excitation,

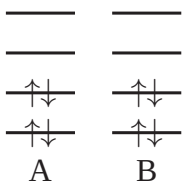

The ground state

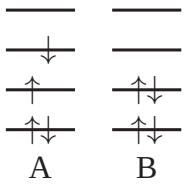

A local excitation, A^*

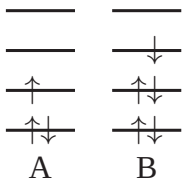

A charge transfer state, A^+B^-

Figure 1: Illustration of classes of excitations.

and for well-separated monomers the excitation energy should be approximately the same in a supermolecule calculation as in calculations for isolated monomers. In the molecular orbital picture being used here both the initial and final orbitals may be delocalised over multiple monomers. In this work no attempt is made to characterise such distributed local excitations further, provided there is no net transfer of electron density from one monomer to another. Distributed local excitations also arise in coupled monomer modelling (see e.g. Novoderezhkin et al.[7]) and are here denoted e.g. A^*B^*.

The second type of excitation is shown in the lower panel of Figure 1, in which an electron from the HOMO of monomer A is excited into the LUMO of monomer B. This state can be described as A^+B^- and is termed a charge transfer

state in this work. This could equally be called an electron transfer state. When performed as a supermolecule calculation, the energy of a local excitation state would be expected to be approximately equal to the energy of the first excited state of A plus the ground state energy of B. On the other hand, the energy of an A^+B^- charge transfer state would be expected to be substantially different to the sum of the energies of the isolated A^+ cation and isolated B^- anion. Higher energy charge transfer states involve excitations of electrons from orbitals other than the HOMO or excitations to virtual orbitals other than the LUMO. Note that only singlet states are considered.

3 Results

The PS II reaction centre and its attendant proteins is far too large to describe in its entirety with accurate electronic structure theory calculations. Thus a series of computational models was built up sequentially. As the models got larger further approximations were introduced, validating the more approximate treatment of larger models against the observed features of the "previous" model. Initially it was confirmed that truncating gas phase chlorophyll at the ester group of the hydrocarbon tail had a negligible effect on the calculated excited states, which principally involve excitations of the conjugated structure of the chlorin ring motif within the chlorophyll. Furthermore, whether the Mg atom of chlorophyll was coordinated only to the nitrogens of the containing ring or additionally to water or histidine ligands was shown to affect the excitation energies by an insignificant amount in the current context (being shifted by 80 meV or less). It was also confirmed that the presence of diffuse functions in the basis set principally shifted the

excitation energies globally. This was determined by comparing calculations with the 6-31+G(d,p) and 6-31G(d,p) basis sets for a dimer of chlorophylls with the truncated hydrocarbon tail. The inclusion of diffuse functions in calculations of larger aggregates of cofactors led to convergence difficulties. (Explicit excitation energies demonstrating these results are given in Table S1 of the Supplementary Information.)

Four models that were used in this work are illustrated in Figure 2. The energies of a range of excited states (relative to the calculated ground state energy) for these and related models are shown in Figure 3. In this and subsequent figures, states are coloured according to their observed character, distinguishing between states that are principally local excitations on individual rings, charge transfer from one of the rings representing P_{D1} or P_{D2} to the other, "forward" charge transfer that shifts electrons toward Q_A or Q_B, "backward" charge transfer that shifts electrons toward or to P_{D1} or P_{D2}, and the special case of forward charge transfer with Q_A as the electron acceptor (yielding Q_A^-). An expected similar state with an excess electron on Q_B was not found, presumably lying at an energy above the calculated set of states. Note that the number of states calculated for each model was not designed to determine a totally consistent manifold of correlatable states as the models developed from right to left in Figure 3, with states allowed to enter or leave the calculated region (from/to higher energies) between models. Between 20 and 45 excited states were calculated, depending on the model.

Figure 3 illustrates that the most significant change in the calculated excitations occurs when dropping the chlorophyll side chains and moving to the idealised chlorin ring model (from 1 to 2 in Figure 3). Aside from a wholesale shift of the excitation energies to larger values, forward and backward charge transfer

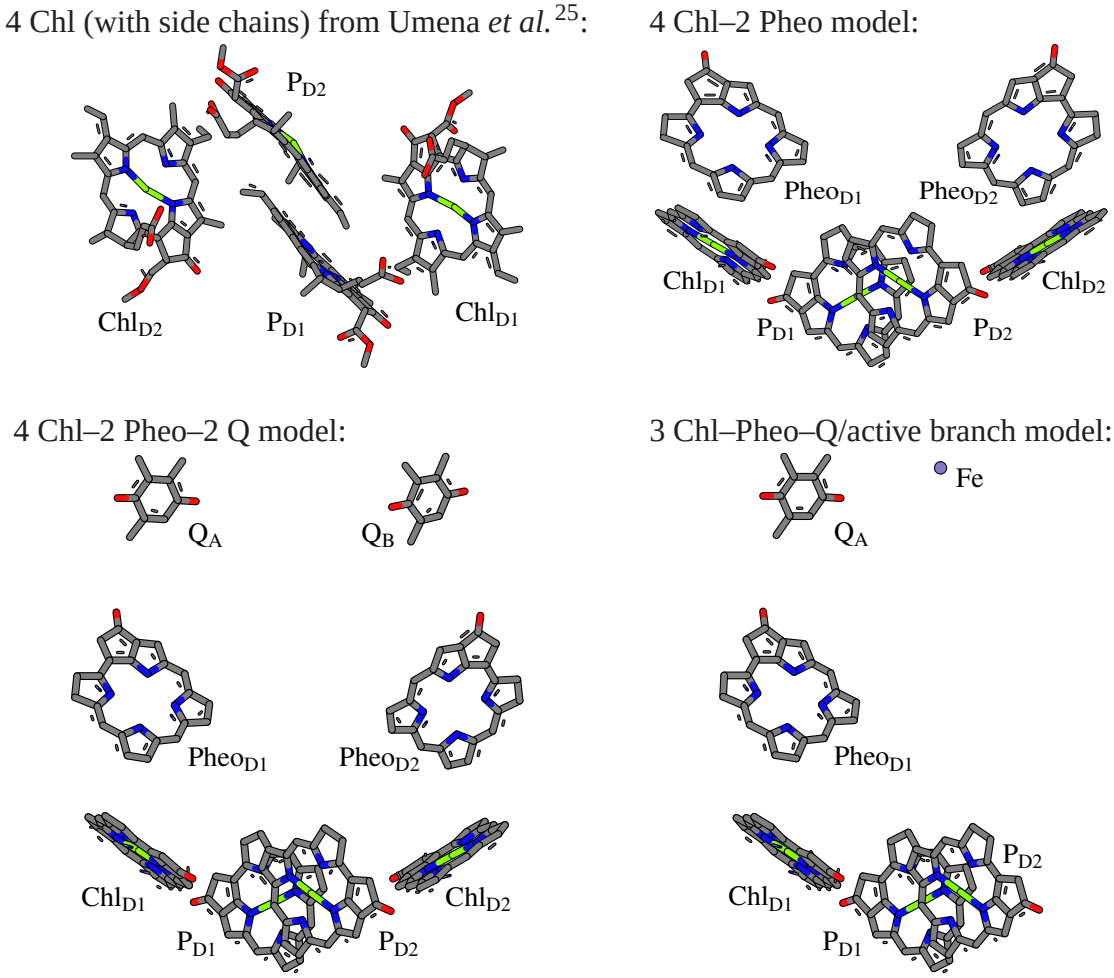

Figure 2: PS II reaction centre cofactor aggregate models. Note that hydrogen atoms are not shown. Note also the 4 Chl structure (top left) is drawn here with a different orientation to the others. In the active branch model (bottom right) the non-heme iron site ("Fe") is the site for a point charge rather than an atom.

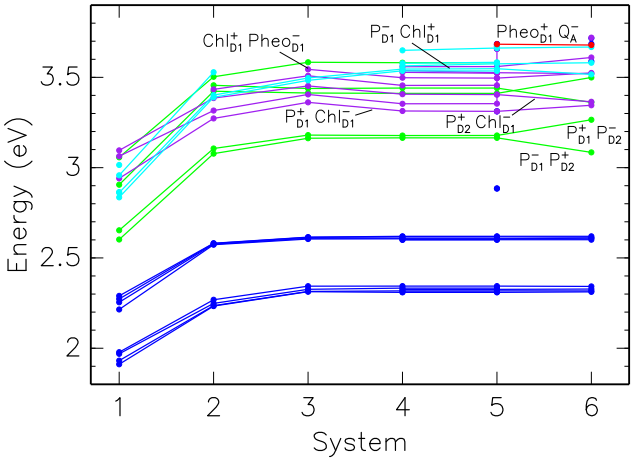

Figure 3: TDDFT (CAM-B3LYP) excitation energies for a range of reaction centre models and basis sets. 1: 4 Chl (with side chains, truncated hydrocarbon tail) from Umena *et al.*[25], 6-31G(d); 2: 4 Chl model, 6-31G(d,p); 3: 4 Chl model, 6-31G; 4: 4 Chl–2 Pheo model, 6-31G; 5: 4 Chl–2 Pheo–2 Q model, 6-31G; 6: 3 Chl–Pheo–Q/active branch model (zero Fe charge), 6-31G. States coloured according to character: local excitations (blue), $P_{D1} \leftrightarrow P_{D2}$ charge transfer (green), "forward" charge transfer (purple), "backward" charge transfer (cyan) and charge transfer to Q_A (red). Note that approximately equivalent states from each side of the cofactor chain (e.g. $P^{+}_{D2}Chl^{-}_{D1}$ and $P^{+}_{D1}Chl^{-}_{D2}$) are connected at the 4 Chl–2 Pheo–2 Q model.

states largely swap positions in the spectrum. The major component of this change is the relaxation from the crystal structure positions of the ring atoms to the relaxed gas phase configuration rather than the neglect of the side chains. In this context one should recall that the crystal structure data is of limited resolution and should be interpreted in conjunction with attendant positional uncertainties and thermal ellipsoids, so this change from the crystal structure model to the idealised chlorin rings models should not be considered to represent an obvious change from the physically real system. Similar work on photosystem I has concluded that the use of crystal structure coordinates degrades the quality of computational results.[18] The major conclusions of this work do not depend on the detailed ordering within the dense regions of the spectrum, and thus these changes do not have a strong impact on the conclusions to be drawn.

The third illustrated model (4 Chl–2 Pheo–2 Q) contained the greatest number of cofactors and might therefore be expected to most closely resemble the behaviour of the reaction centre. Not surprisingly, this was also the most computationally expensive model to perform calculations on. For that reason the fourth model, denoted the active branch model, was preferred for most of the calculations performed. Figure 3 illustrates that the principle effect of changing to the smaller, active branch model was to substantially increase the energy difference between the $P_{D1}^{+}P_{D2}^{-}$ and $P_{D1}^{-}P_{D2}^{+}$ states (shown in green in Figure 3).

Local excitations of Q_A were resolved by the calculations on the 4 Chl–2 Pheo–2 Q model. The lowest was at an energy intermediate between the second set of chlorin-based local excitations and the lowest $P_{D1} \leftrightarrow P_{D2}$ charge transfer states, visible as a blue dot at 2.9 eV in Figure 3. Calculations on the methylated benzoquinone used to represent Q_A/Q_B confirms that this local excitation would

be expected at around that energy. This state is not resolved in the calculations on the active branch model. Despite the range of calculations performed on the active branch model, only one other calculation resolved this state (visible at Fe charge $+0.1$ in Figure 4). Determining why the TDDFT calculations usually missed this state is beyond the scope of the current study, becoming a much more fundamental question about the implementation of quantum chemistry methods.

It is worth noting that the characterisation of excitations according to their principle character does not imply that these are "pure" states. Indeed, in most cases what is given here as the principle character was accompanied by smaller amounts of what would be characterised as other types of excitation. For example, the lowest energy charge transfer state of the active site model has been characterised in this work as the $P_{D1}^{-}P_{D2}^{+}$ state. But the transition density for excitation to this state comprises only around 92% of clearly $P_{D2} \rightarrow P_{D1}$ electron transfer (expressed in terms of ground state orbitals). The next largest component was clearly P_{D1} HOMO to LUMO excitation. This is consistent with spectroscopic evidence of mixed character states comprising both local excitation and charge transfer nature.[7,26] The P_{D1} and P_{D2} cofactors were particularly tightly coupled, with states involving charge transfer to or from one of these cofactors often containing significant character of charge transfer to or from the other.

Initial work on chlorophyll dimers indicated a strong dependence of the energies of charge transfer states on external electric fields. This is explicitly demonstrated in Figure S1 of the Supplementary Information and is readily understood as a Stark effect.[27] This suggests the electrostatic environment surrounding the cofactors and charge transfer elements of the reaction centre may have a significant effect. One of the most obvious persistent electrostatic elements surrounding

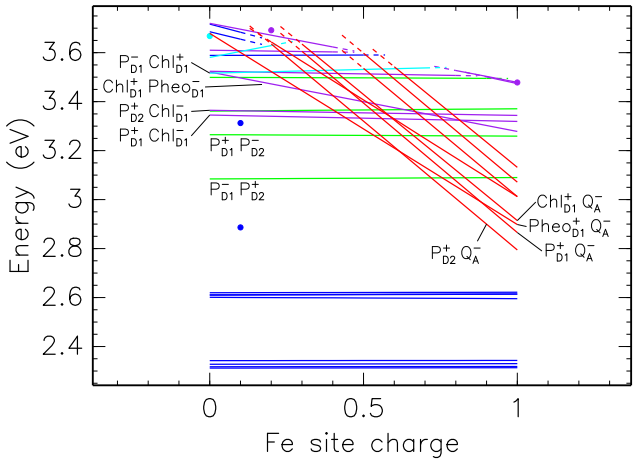

Figure 4: Excitation energies as a function of the charge located at the Fe site (in increments of 0.1) for the active branch model. Same colour scheme as Fig. 3.

the modelled reaction centre cofactors is the so-called non-heme iron. This is located roughly between Q_A and Q_B. As this Fe(II) atom is ligated to a bicarbonate anion, the effective charge of this site is expected to be around $+1$. To investigate the effect of such a charge, calculations were performed with a point charge of up to $+1$ located at the position of the non-heme iron. The resultant excitation energies are shown in Figure 4.

Figure 4 shows that the effect of such a static charge is dramatic. Most local excitation energies and charge transfer states were only weakly affected by the Fe static charge. However, charge transfer states involving an electron transferred to the Q_A site were strongly stabilised, with energies decreasing linearly with the Fe charge. Only one such Q_A^- state was found in the first 25 excited states for the zero charge model. When the Fe site charge was increased to $+1$, eight of the nine lowest energy charge transfer states featured Q_A^-, with the lowest almost 1 eV lower in energy than the lowest zero Fe charge Q_A^- state. In these states the hole could be located on any of the chlorin rings.

It is worth noting that one should not expect the shifts in the excitation energies calculated here as a function of the charge on the Fe site to be simply related to spectra obtained with Stark spectroscopy.[26,27] While the physical effects of the electric field from a localised net charge on an internal region and of the uniform field applied externally in a Stark spectroscopy experiment are essentially the same, the effects of the former cannot be simply removed by the latter. Strong localisation of charge therefore screens nearby regions from being probed effectively by external fields.

As the catalytic water oxidation photocycle continues, it is thought that electrons accumulate at the Q_B site (having transferred from Q_A via superexchange[28]) before being transported away from the reaction centre, possibly mediated by Q_B^{n-} translational motion[29] but ultimately resulting in hydrogenation of the plastoquinone.[30] For this picture to be realistic, the primary charge separation and migration of charge to Q_A must operate in the presence of negative charge located in the vicinity of Q_B, although such charges may well be neutralised by the motion of other charge-carrying groups[31] and recent modelling suggests that the protonation occurs sequentially *in situ*.[32] An accumulation of negative charge on Q_B may be expected to interfere with any Q_A^- stabilising effect of the Fe site charge.

As a test, calculations were performed with both a $+1$ point charge at the Fe site and -1 point charge located at the centre of the Q_B position from the 1.9 Å crystal structure. The effect of additional negative charge in the vicinity of Q_B was indeed to destabilise the Q_A^- charge transfer states. These move approximately 0.3 eV higher to energies above the $P_{D1}^- P_{D2}^+$ state near 3.1 eV. Most of the lowest lying charge transfer states were still Q_A^--containing states despite their destabilisation. If the Q_B^- charge is moved further away from the Fe site, as might

be expected in the event of a more mobile Q_B group, the Q_A^- charge transfer states decrease in energy to about 0.1 eV above the positions shown in Figure 4.

The electric field felt a distance away from an electric charge such as that expected to be located in the vicinity of the non-heme iron depends on the polarisability of the environment. The protein environment surrounding the active elements of the photosystem II reaction centre is to some extent polarisable. The modelling of the effect of polarisable environments is a complex topic, with a range of approaches being applied in practice without a clear route to the most appropriate treatment for any particular problem. This is exacerbated in protein environments, where the effective permittivity is spatially inhomogeneous.[33] To explore some of the effects of the polarisability of the protein environment on the excitation energies calculated in this work, calculations were performed with a relative permittivity (dielectric constant) greater than 1 (the vacuum value) within the PCM approach. The results are shown in Figure 5 for zero charge at the Fe site (corresponding to the left edge of Figure 4) and in Figure 6 for a charge of $+1$ at the Fe site (corresponding to the right edge of Figure 4).

In both cases the relative energies of the local excitation states decrease with increasing polarisability, whereas non-Q_A charge transfer states may move up or down. Q_A^- charge transfer states all decrease in energy as the polarisability increases, before becoming quite insensitive to the dielectric constant above around $\varepsilon = 4$ to $\varepsilon = 6$. At still higher permittivities (beyond what is shown in Figures 5 and 6) the behaviour evident in these figures continues, with the excitation energy curves getting progressively flatter and more independent of ε as ε increases.

Not all of the states illustrated in Figures 4–6 are optically active. Indeed, the majority are not. Some calculated oscillator strengths for transitions to these

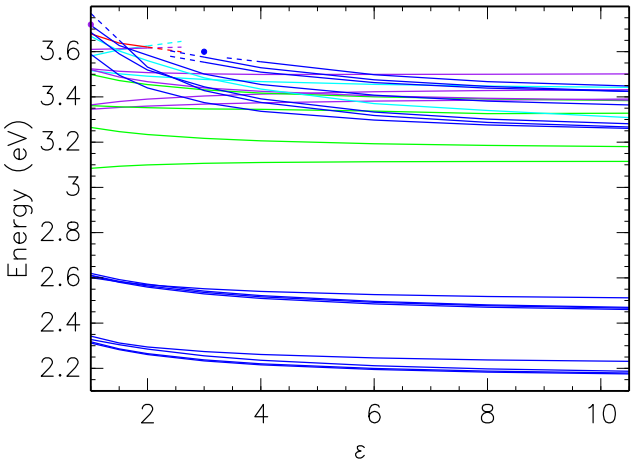

Figure 5: Excitation energies as a function of the dielectric constant of the environment for the active branch model, when there is no charge at the non-heme iron site (left edge of Fig. 4). Same colour scheme as Fig. 3.

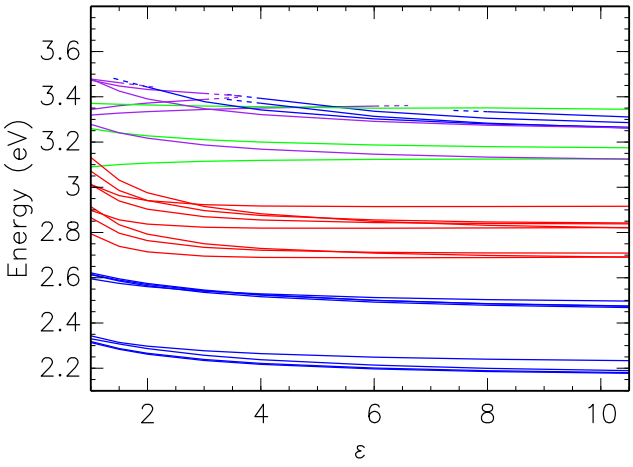

Figure 6: Excitation energies as a function of the dielectric constant of the environment for the active branch model, when there is a +1 charge at the non-heme iron site (right edge of Fig. 4). Same colour scheme as Fig. 3.

Table 1: Calculated active branch model excitation oscillator strengths

	Zero charge	Fe site +1
$Chl^*_{D1}Pheo^*_{D1}$	0.38	0.40
$P^*_{D1}P^*_{D2}$	0.18	0.17
$P^*_{D2}Pheo^*_{D1}$	0.021	0.019
$P^*_{D1}P^*_{D2}Chl^*_{D1}$	0.049	0.049
$Pheo^*_{D1}$	0.042	0.040
P^*_{D1}	0.047	0.043
P^*_{D2}	0.034	0.036
Chl^*_{D1}	0.054	0.057
$P^-_{D1}P^+_{D2}$	0.013	0.013
$P^+_{D1}P^-_{D2}$	0.0093	0.0086
$P^-_{D1}P^+_{D2}$	0.010	0.11
$P^*_{D1}P^*_{D2}$	0.71	–
Chl^*_{D1}	0.36	–
$Pheo^*_{D1}$	1.3	–
$Chl^+_{D1}Pheo^-_{D1}$	0.19	–

states are given in Table 1. All states for the active branch model without (Zero charge) and with (Fe site +1) a point charge located at the position of the non-heme iron that exhibited a non-negligible oscillator strength are shown. (The last four optically active states shown for zero Fe charge correlate with states above the lowest 25 excited states calculated for a +1 Fe site charge.) Generally only chlorin ring local excitations and $P_{D1} \leftrightarrow P_{D2}$ charge transfer states were shown to be optically active. There is experimental support for both local excitations and primary charge transfer being directly optically accessible.[34] The exception to this categorisation is the $Chl^+_{D1}Pheo^-_{D1}$ state, which lies high in energy above 3.7 eV. Note that these active branch model results are completely consistent with calculations on all other cofactor supermolecule models.

4 Discussion

The optically-active part of the PS II reaction centre is known as P680, reflecting the associated adsorption feature at a wavelength of 680 nm, corresponding to photon energies around 1.8 eV. It is then notable that the lowest vertical excitation energies for the four chlorophyll model with side chains were calculated to lie around 1.9 eV (Figure 3). It is not expected that such a truncated, static, gas phase model should yield excitation energies exactly matching experimental adsorption energies, but they should be comparable. As shown in Figure 3, idealising the chlorophyll cofactors to chlorin rings principally acted to raise the energy of the local excitation states relative to the ground state, as did, to a lesser extent, reducing the size of the basis set used for the calculations. As indicated in Figures 5 and 6, removing the modelled cofactors from a polarisable medium also raises most of the the excitation energies.

The oscillator strengths of Table 1 clearly indicate that only states that are principally local excitation and $P_{D1} \leftrightarrow P_{D2}$ charge transfer states will be directly excited by incident radiation at less than around 3.5 eV (350 nm), rather than charge transfer states directly transferring electrons to any of the other cofactors. In particular, the charge transfer states featuring Q_A^- all exhibited zero oscillator strength irrespective of being lowered in energy by the presence of positive charge at the non-heme iron site and by dielectric effects. This supports the view that the transfer of an electron to Q_A (and subsequently to Q_B to allow further photosynthetic reactions) following excitation of P680 and primary charge separation requires a sequence of electron transfer steps.

Such electron transfer events are often described using Marcus-Hush theory.

In this context, the vertical excitation energies calculated in this work can be interpreted as a measure of the reorganisation energy, often denoted λ. Such an interpretation lends particular weight to the stabilising effect of the non-heme iron charge on the Q_A^--containing states, as the Marcus-Hush electron transfer rate decreases exponentially with increasing λ. However, the rate also decreases exponentially with the electron transfer distance. Of the possible transitions between the charge transfer states calculated in this work, directly transitioning to a $P_{D1}^+Q_A^-$ or $P_{D2}^+Q_A^-$ state (which has the lowest suggested λ energy) corresponds to the longest distance electron transfer.

More direct modelling of such electron transfer events, essentially hopping from one excited state of the cofactor aggregation to another, is beyond the scope of the current work. Such modelling requires consideration of excited state geometrical relaxation and vibronic coupling, whereas all calculations performed in the current study were for supermolecules fixed at the geometries implied by the XRD crystal structure of Umena *et al.*[25] Recent developments in the construction of quasidiabatic potential energy functions from *ab initio* data[35–37] are likely to make flexible, high dimensional, quantum-chemistry-derived reaction centre models accessible in the foreseeable future. Parallel developments in quantum dynamics methodologies[38–41] suggest that a fully quantum mechanical treatment of the electron transfer process, while onerous, is possible. Such a treatment would allow the treatment of transitions between the local excitation states without explicit dipole-dipole coupling approximations.

An indicative measure of the relative likelihood of rapid transitions to "forward" charge transfer states can be gleaned in the current work from the forces on the atoms calculated for each excited state. For the active branch model with

any Fe site charge the forces on the atoms for charge transfer excited states were around twice as large as those for local excitation states, with the latter being approximately the same as for the ground state. (Recall that the atoms in the model are not relaxed but held at the positions implied by the XRD crystal structure.) Assuming that the potential energy is adequately described as a harmonic function and that the force constants are similar in the different states, this suggests that the charge transfer excited states are around twice as far from their equilibrium geometries as the local excitation or ground states. This in turn suggests that the vibrational density of states in the charge transfer states would be considerably larger than for the local excitation or ground states. Thus applying a Fermi golden rule argument suggests transfer of the system from a local excitation state to a charge transfer state should be rapid. While this argument can be considered indicative at best, it is at some odds with the coupling coefficients used in published modelling.[9–11] The current results suggest that all the local excitation states should couple strongly to charge transfer states, whereas a more sparse coupling between particular local excitation states and charge transfer states arises in existing modelling. However, rapid electron transfer within the reaction centre complex is supported by modelling.[42]

Such discussions do not include the transfer of excitations from antenna complexes. Energy transfer from adjacent cofactors could conceivably excite charge transfer states directly, without passing initially through a reaction centre local excitation state. Multiple excitation pathways being active simultaneously is supported by existing modelling.[10]

It has recently been suggested that the site energies of $Pheo_{D1}$ and $Pheo_{D2}$ should be considered to be significantly different, with peak absorbences sepa-

rated by around 25 meV.[14] The 4 Chl–2 Pheo and 4 Chl–2 Pheo–2 Q models explicitly contain both $Pheo_{D1}$ and $Pheo_{D2}$. In these models excitation energies to states involving local excitations of or charge transfer to $Pheo_{D1}$ or $Pheo_{D2}$ differ by at most 10 meV, with many such states being substantially closer in energy. These results neither directly support nor refute $Pheo_{D1}$ and $Pheo_{D2}$ having different site energies.

The computational resources required to perform these calculations were modest. Most individual calculations were completed within a few hours on a 16 core node based on Xeon processors. The memory requirements were likewise achievable, with most calculations requiring less than 50 GB of RAM for 25 excited states, even with the duplication implied by running Gaussian 09 in parallel.

5 Conclusion

This work demonstrates that explicit consideration of PS II reaction centre in a unified electronic structure theory calculation should now be considered to be easily within the reach of current computing systems. While the basis sets used in the current work were relatively modest, future kinetic modelling should incorporate the explicit calculation of coupling coefficients between aggregates of cofactors.

The electronic structure theory calculations performed here support the conclusion that the primary charge separation in the PS II reaction centre occurs in the $P_{D1}P_{D2}$ pair. However, it is worth noting that the $P^{+}_{D1}Q^{-}_{A}$ and $P^{+}_{D2}Q^{-}_{A}$ states were found to be substantially lower in energy than $P_{D1} \leftrightarrow P_{D2}$ charge transfer states under the influence of a positive charge located at the non-heme iron site. Direct transfer to this state following chlorophyll/pheophytin excitation cannot be

ruled out based on this work.

A notable feature of the calculations performed here that is not regularly incorporated in existing modelling is the presence of multiple local excitation states for each cofactor, at energies substantially lower than the charge transfer states (at least at the geometries considered in this work). Similarly, multiple states with the same charge transfer character were found without going to very high excitation energies. Such states could act as "gateway" states, reducing the threshold energy for subsequent charge transfer (but at a reduced rate) for any particular set of coupling coefficients.

Finally, this work demonstrates that consideration of the electrostatic environment around the electronically-active cofactors is vital for realistic modelling. The energies of the relevant excited states are changed qualitatively by the electrostatic fields imparted by the surrounding proteins and related structures.

Acknowledgement

This work was supported by the NCI National Facility at the ANU. The author would like to thank Elmars Krausz, Ron Pace and Alfred Holzwarth for useful discussions. Some initial exploratory calculations were performed by Sicheng Ma.

References

[1] *Photosystem II: The light-driven water:plastoquinone oxidoreductase*, ed. T. J. Wydrzynski and K. Satoh, Springer, Dordrecht, 2005, vol. 22.

[2] G. Renger, *J. Photochem. Photobiol. B: Biol.*, 2011, **104**, 35.

[3] D. G. Nocera, *Acc. Chem. Res.*, 2012, **45**, 767.

[4] T. Renger and E. Schlodder, *J. Photochem. Photobiol. B: Biol.*, 2011, **104**, 126.

[5] V. I. Novoderezhkin, E. G. Andrizhiyevskaya, J. P. Dekker and R. van Grondelle, *Biophys. J.*, 2005, **89**, 1464.

[6] G. Raszewski, W. Saenger and T. Renger, *Biophys. J.*, 2005, **88**, 986.

[7] V. I. Novoderezhkin, J. P. Dekker and R. van Grondelle, *Biophys. J.*, 2007, **93**, 1293.

[8] G. Raszewski, B. A. Diner, E. Schlodder and T. Renger, *Biophys. J.*, 2008, **95**, 105.

[9] D. Abramavicius and S. Mukamel, *J. Chem. Phys.*, 2010, **133**, 184501.

[10] V. I. Novoderezhkin, E. Romero, J. P. Dekker and R. van Grondelle, *ChemPhysChem*, 2011, **12**, 681.

[11] A. Gelzinis, L. Valkunas, F. D. Fuller, J. P. Ogilvie, S. Mukamel and D. Abramavicius, *New J. Phys.*, 2013, **15**, 075013.

[12] J. C. Chang, *J. Chem. Phys.*, 1977, **67**, 3901.

[13] M. E. Madjet, A. Abdurahman and T. Renger, *J. Phys. Chem. B*, 2006, **110**, 17268.

[14] K. Acharya, B. Neupane, V. Zazubovich, R. T. Sayre, R. Picorel, M. Seibert and R. Jankowiak, *J. Phys. Chem. B*, 2012, **116**, 3890.

[15] M. Wormit, P. H. P. Harbach, J. M. Mewes, S. Amarie, J. Wachtveitl and A. Dreuw, *Biochim. Biophys. Acta*, 2009, **1787**, 738.

[16] C. König, N. Schlüter and J. Neugebauer, *J. Chem. Phys.*, 2013, **138**, 034104.

[17] C. König and J. Neugebauer, *ChemPhysChem*, 2012, **13**, 386.

[18] S. Yin, M. G. Dahlbom, P. J. Canfield, N. S. Hush, R. Kobayashi and J. R. Reimers, *J. Phys. Chem. B*, 2007, **111**, 9923.

[19] M. J. Frisch, G. W. Trucks, H. B. Schlegel, G. E. Scuseria, M. A. Robb, J. R. Cheeseman, G. Scalmani, V. Barone, B. Mennucci, G. A. Petersson, H. Nakatsuji, M. Caricato, X. Li, H. P. Hratchian, A. F. Izmaylov, J. Bloino, G. Zheng, J. L. Sonnenberg, M. Hada, M. Ehara, K. Toyota, R. Fukuda, J. Hasegawa, M. Ishida, T. Nakajima, Y. Honda, O. Kitao, H. Nakai, T. Vreven, J. A. Montgomery, Jr, J. E. Peralta, F. Ogliaro, M. Bearpark, J. J. Heyd, E. Brothers, K. N. Kudin, V. N. Staroverov, T. Keith, R. Kobayashi, J. Normand, K. Raghavachari, A. Rendell, J. C. Burant, S. S. Iyengar, J. Tomasi, M. Cossi, N. Rega, J. M. Millam, M. Klene, J. E. Knox, J. B. Cross, V. Bakken, C. Adamo, J. Jaramillo, R. Gomperts, R. E. Stratmann, O. Yazyev, A. J. Austin, R. Cammi, C. Pomelli, J. W. Ochterski, R. L. Martin, K. Morokuma, V. G. Zakrzewski, G. A. Voth, P. Salvador, J. J. Dannenberg, S. Dapprich, A. D. Daniels, O. Farkas, J. B. Foresman, J. V. Ortiz,

J. Cioslowski and D. J. Fox, *Gaussian 09*, Gaussian, Inc., Wallingford CT, 2013.

[20] T. Yanai, D. P. Tew and N. C. Handy, *Chem. Phys. Lett.*, 2004, **393**, 51.

[21] R. Kobayashi and R. D. Amos, *Chem. Phys. Lett.*, 2006, **420**, 106.

[22] Z.-L. Cai, M. J. Crossley, J. R. Reimers, R. Kobayashi and R. D. Amos, *J. Phys. Chem. B*, 2006, **110**, 15624.

[23] J. R. Reimers, Z.-L. Cai, R. Kobayashi, M. Rätsep, A. Freiberg and E. Krausz, *Sci. Rep.*, 2013, **3**, 2761.

[24] J. Tomasi, B. Mennucci and R. Cammi, *Chem. Rev.*, 2005, **105**, 2999.

[25] Y. Umena, K. Kawakami, J.-R. Shen and N. Kamiya, *Nature*, 2011, **473**, 55.

[26] E. Romero, B. A. Diner, P. J. Nixon, W. J. Coleman, J. P. Dekker and R. van Grondelle, *Biophys. J.*, 2012, **103**, 185.

[27] S. G. Boxer, *J. Phys. Chem. B*, 2009, **113**, 2972.

[28] S. Fletcher, *J. Solid State Electrochem.*, 2014, DOI 10.1007/s10008-014-2567-z.

[29] A. Guskov, J. Kern, A. Gabdulkhakov, M. Broser, A. Zouni and W. Saenger, *Nature Struct. Molec. Biol.*, 2009, **16**, 334.

[30] F. Müh, C. Glöckner, J. Hellmich and A. Zouni, *Biochim. Biophys. Acta*, 2012, **1817**, 44.

[31] R. Hienenvadel, S. Grzybek, C. Fogel, W. Kreutz, M. Y. Okamura, M. L. Paddock, J. Breton, E. Nabedryk and W. Mäntele, *Biochem.*, 1995, **34**, 2832.

[32] K. Saito, A. W. Rutherford and H. Ishikita, *Proc. Nat. Acad. Sci.*, 2013, **110**, 954.

[33] A. Warshel, P. K. Sharma, M. Kato and W. W. Parson, *Biochim. Biophys. Acta*, 2006, **1764**, 1647.

[34] J. L. Hughes, B. J. Prince, E. Krausz, P. J. Smith, R. J. Pace and H. Riesen, *J. Phys. Chem. B*, 2004, **108**, 10428.

[35] O. Godsi, C. R. Evenhuis and M. A. Collins, *J. Chem. Phys.*, 2006, **125**, 104105.

[36] C. Evenhuis and T. J. Martínez, *J. Chem. Phys.*, 2011, **135**, 224110.

[37] D. R. Yarkony, *Chem. Rev.*, 2012, **112**, 481.

[38] M. H. Beck, A. Jäckle, G. A. Worth and H.-D. Meyer, *Phys. Rep.*, 2000, **324**, 1.

[39] G. A. Worth, M. A. Robb and I. Burghardt, *Faraday Discuss.*, 2004, **127**, 307.

[40] T. J. Frankcombe, M. A. Collins and G. A. Worth, *Chem. Phys. Lett.*, 2010, **489**, 242.

[41] W. Koch and T. J. Frankcombe, *Phys. Rev. Lett.*, 2013, **110**, 263202.

[42] G. Raszewski and T. Renger, *J. Am. Chem. Soc.*, 2008, **130**, 4431.

TOC graphic

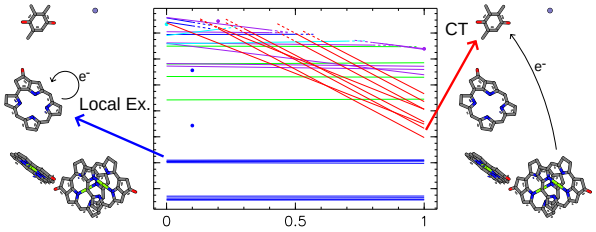

The excited states of the photosystem II reaction centre cofactors have been calculated as a single “supermolecule”. Charge transfer states are shown to be dependent on electrostatic environment.